Modeling Fluid Dynamics in Porous Media: A Pore-Scale Flow Analysis

Haval Kukha Hawez*, Frya R. Asaad, Abdulla N. Suleiman, Ahmed S. Khorsheed

Department of Petroleum Engineering, Faculty of Engineering, Koya University, Koya, KOY45, Kurdistan Region - F.R. Iraq.

* Correspondence author: haval.hawez@koyauniversity.org

Abstract

This study investigates single-phase fluid flow in porous media using advanced numerical methods, with a focus on pore-scale dynamics, to address the limitations of traditional models, such as Darcy's law. The research utilizes the Creeping Flow interface and the Brinkman equation to analyze velocity and pressure distributions in heterogeneous porous media. Qualitative results indicate the presence of distinct flow patterns characterized by high-velocity areas (up to 8×10^{-5} m/s) localized in narrow, interconnected channels. At the same time, stationary zones have very little flow, which shows how pore shape affects the paths that fluids take. The Brinkman equation accounts for viscous shear effects and exhibits smoother changes in velocity (0–1.8×10^{-5} m/s) compared to the Creeping Flow model, which predicts sharper gradients. Pressure distributions reveal significant decreases (0.39–6.91 Pa) in constricted areas, demonstrating the impact of tortuosity and connectedness on flow resistance. A quantitative study shows that the Creeping Flow model is most effective for systems with low permeability, whereas the Brinkman equation performs better for systems with intermediate flow rates. These results help us better understand how fluids move across porous networks, which is beneficial for applications such as increasing oil production and removing contaminants. The study bridges theoretical modeling and practical

scenarios, providing a foundation for optimizing resource management and sustainable extraction techniques.

Keywords**:** Pore-scale flow, Creeping flow, Brinkman equation, Numerical fluid dynamics.

1. Introduction

Fluid flow through a porous medium is a fundamental physical phenomenon that spans various fields of science and engineering, including hydrology, petroleum engineering, and environmental science. The capacity of fluid behavior modeling and full-scale prediction in porous media holds a significant place in real-world applications, such as groundwater management, oil recovery, and pollution control. The interlaced geometrical parameters of the porous media, which have different pore structures ranging from simple to complex, are well recognized. These structural features rank first among the key factors determining fluid flow and its movement through materials, as well as the primary characteristics such as permeability and diffusion. Crucial parameters, including pore geometry, fluid viscosity, and the interfacial properties of the solid matrix with the fluid, influence the behavior of fluids in porous media. All these aspects contribute to the prediction of flow patterns, which is a key issue in the effective extraction of resources and, thus, in the successful extraction of resources. In a calibrated manner, petrophysical parameters help develop more effective methodologies for oil and gas recovery and environmental science, as well as forecasting contaminant movement through soil and groundwater systems (H. K. Hawez et al., 2021; Young and Kabala, 2024).

The movement of fluids at the pore scale is different differs from the behavior observed in the large-scale movement of fluids. The fluid flow and the structure of the porous media are complicated on this scale, which leads to strange flow patterns. The medium's complex arrangement of pores and mouths gives rise to distinct flow patterns (Hawez et al., 2024; Singh et al., 2017). The flow pattern in the intricate pore structures can generally be categorized into two main types: single-phase and multi-phase flow. Single-phase flow refers to the movement of a single fluid phase through porous media, such as water or oil, in a system where the fluid is not separated into distinct phases (Blunt, 2001). Darcy's law typically governs this type of flow, an equation that defines the relationship between the pressure decrease across porous media and the volumetric flow rate. Darcy's law is applied in flow analysis through porous media because it gives a relatively straightforward means of estimating flow characteristics under given conditions (Asim and Hawez, 2024). This implies that they always have a flow with constant fluid viscosity and constant permeability of the medium. Although Darcy's law is adequate for single-phase flow in comparatively homogeneous media, it is less effective in multiple-phase flow, where more than one phase of the fluid (such as oil and water) may be present in the same porous structure (H. Hawez et al., 2021). It is crucial to effectively characterize and distinguish between these flow regimes to accurately estimate and extrapolate fluid phase behavior in porous media.

In practical problems, it is almost always necessary to consider multiphase flow, which occurs when more than one fluid is present in the porous medium (Carrillo et al., 2020). One kind of such a system is an oil-water flow, characteristic of petroleum engineering. In these cases, the flow behavior is much more complex due to the interphase transfer between the two phases of the fluids, forces due to the capillary pressures related to the surface tension at the interfaces between the fluids, and the interfacial tensions that are the forces at the boundary between different phases are of much importance (Hawez and Asim, 2024a). These forces may help define the distribution of phases within the pores, which in turn influence factors such as fluid mobility, pressure distribution, and flow. These phenomena result from the complexity of interactions within fluid phases at small scales, including the formation of fluid films, snap-off events, and the confinement of liquids within pore structures. Although these events are of little significance at the microscale, they can substantially affect the behavior of fluid flow dynamics and fluid mobility. This type of behavior is poorly captured by traditional models, which require higher-order techniques for modeling (Anvari and Turzó, 2022; Jettestuen et al., 2013). These models must be reasonably detailed in terms of flow dynamics and fluid behavior in such systems, taking into account capillary forces, interfacial tensions, and pore geometry. Only advanced models can make such a deep understanding.

Recent improvements in numerical techniques, notably the Lattice Boltzmann Method and pore-scale network modeling, have provided new opportunities for simulating and investigating fluid flow dynamics through porous media (Liu and Wu, 2016). This represents a significant step forward in our understanding of how complex flow behaves at the pore scale. It makes simulations far more detailed and accurate than they were before. For example, the solution of the Boltzmann transport equation on a microscale using the Lattice Boltzmann Method provides a solid basis for simulating flow, thereby representing the flow of fluids through porous media more realistically (Montessori et al., 2016).

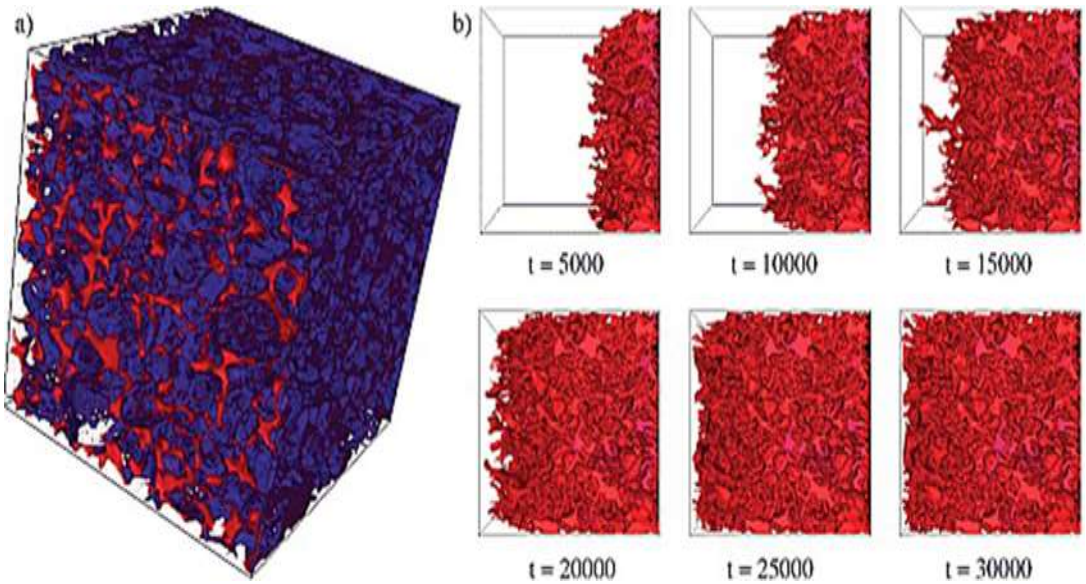

Fig. 1. Lattice Boltzmann simulation of fluid-fluid displacement in a porous medium. (a) A visualization of a 4.9 µm resolution X-ray tomography image of a Benthheimer sandstone with the mineral phase in blue and the pore space in red. (b) Six stages in a lattice (Harting et al., 2005).

Similarly, pore-scale network modeling enables the simulation of a material's complex pore structure, providing detailed insights into the interaction of fluids with that structure under various conditions. It is all of this that improves not only the accuracy of flow forecasting but also deepens knowledge in the areas of multiphase flow, capillary pressure, and fluid entrapment (Joekar-Niasar et al., 2012; Soulaine et al., 2018).

The dynamics of the transport of colloids within porous media are considerably complicated by the fact that colloidal particles may substantially change the fluid behavior inside the system. Nanometre-sized to micrometer-sized entities interact with the fluid and the porous structure, influencing the fluid motion within the medium, and they can also alter flow properties, such as viscosity and fluid-wall interaction (Sochi, 2010; Soulaine et al., 2018). The migration of colloids in porous media can result in their eventual retention or entrapment at a specific location, which in turn affects the overall transport dynamics. The breakthrough curve, plotted against time for an arriving solute at any location in the system, may also be altered through this interaction between the colloids and the pore structure (Kumar et al., 2022; Sun et al., 2024).

Moreover, colloidal particles and pore surfaces affect fluid flow across porous media. These interactions change flow pathways and lower permeability. Colloids and pore walls can entirely or partially limit pore channels, inhibiting fluid passage (Figueiredo et al., 2015). For example, the interactions of the colloidal particles with the pore walls may block or partially restrict some channels of the pores, impeding the free flow of the fluid (Auset and Keller, 2004). The obstructions reduce the effective permeability of the medium, thereby reducing the passage of fluids and giving rise to nonlinear flow behavior patterns where the pressure and flow rate are no longer related through the simple linear trends described by Darcy's law (Menke et al., 2022). Instead, the flow becomes more complex and often encounters sudden changes that can render it less predictable. In dynamics, the key point is that most complications in multiphase systems arise due to interactions among different fluid phases. Interaction among these phases can generate numerous phenomena that may significantly impact system behavior, as illustrated in Fig. 2 (Sivapalan and Blöschl, 2015).

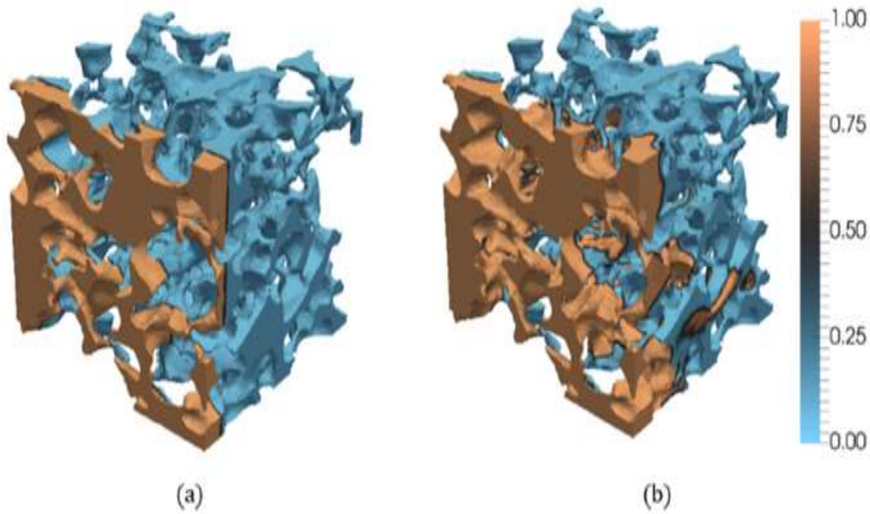

Fig. 2. Fluid distribution of the non-wetting phase during drainage. The brown color indicates the non-wetting phase (i.e., oil), while the blue color is the wetting phase (i.e., water). (a)At initial conditions, oil occupied 14% of the pore space from the inlet (Wu et al., 2022).

The fluid properties in these systems are not considered fixed; instead, they depend upon factors such as capillary pressures, interfacial tensions, and saturation states. Capillary pressures, originating from the curvature of interfaces among different fluid phases, can be disposed of favorably toward fluid migration and may determine the distribution of these phases in a porous medium (Anvari and Turzó, 2022). Interfacial stresses act at fluid phase interfaces. They are essential for fluid-solid interactions in the porous medium. The saturation conditions and the amounts of each phase in the system depend on flow conditions. Such factors may vary considerably along the flow, resulting in nonlinear characteristics for fluid behavior (Hawez and Asim, 2024b; Herrera-Hernández et al., 2023). Such properties will be modified as the system fluctuates owing to pressure, flow rates, or fluid distribution, making it even harder to predict and control such a multiphase flow dynamical system (Zheng et al., 2017). The interaction between all these elements and how they change over time is essential for a good multiphase flow model in enhanced oil recovery.

Accurate modeling of multiple fluid interactions in detail enables scholars to predict the pathways the fluid takes and the paths that pollutants are likely to follow, as well as to identify the most efficient methods for their removal or fixation. This would establish the necessary basis for devising specific measures of remediation with minimal ecological disturbance yet highly effective in removing contaminants; such methods may involve bioremediation approaches, physical barriers, and enhanced flushing techniques (Fopa et al., 2023; Hughes and Blunt, 2001). Improved modeling approaches are badly needed to support the design of engineered systems that depend fundamentally on complex fluid dynamics and high recoveries (Hawez and Ahmed, 2014). This is particularly true in heterogeneous reservoirs, where differences in the development of pore architecture and fluid distribution can render conventional models invalid. Classical models cannot predict fluid dynamics in complex systems with high accuracy due to the non-homogeneities of the porous medium, such as non-uniformly sized pores, connectivity, and even heterogeneity within the reservoir itself. In contrast, state-of-the-art pore-scale models capture all these intricacies while simulating fluid dynamics on a microscale and, therefore, make more realistic predictions of the interaction of fluids with the pore network (Egya et al., 2019; Ekechukwu et al., 2024; Rabbani et al., 2021). These models may lead to more effective extraction methods, improving recovery rates without increasing environmental impact. Models will accurately describe reservoir variability. Thus, insights are essential for creating sustainable resource management systems. This is consistent with the review of the available literature and the use of advanced modeling techniques, which tend to illuminate the real fluid behavior, as it is the question of how much flow conditions and the nature of the pores influence it. These insights provide a solid foundation for developing more effective models, which in turn advance fields such as groundwater remediation, enhanced oil recovery (EOR), and environmental science.

This paper aims to apply modern mathematical tools for modeling multiphase fluid flow in porous media and to enhance the understanding of fluid dynamics in complex systems at the pore scale by developing a model that bridges theory and application. The primary objective is to improve resource management, deliver more accurate forecasts, and facilitate the development of more effective recovery plans applicable in real-world scenarios.

2. Methodology

Various approaches must be employed to achieve the goals of this study, as outlined in the research objectives presented in the preceding chapter. Computational fluid dynamics is one approach for analyzing flow at the pore-scale level. In this chapter, the scope of work for each approach has been determined.

2.1. Geometry

The geometry of this model is based on scanning electron microscope (SEM) images of thinly sliced rock sections, as shown in Fig. 3. This example is from pore-scale flow experiments conducted by the University of California (Auset and Keller, 2004; Sirivithayapakorn and Keller, 2003).

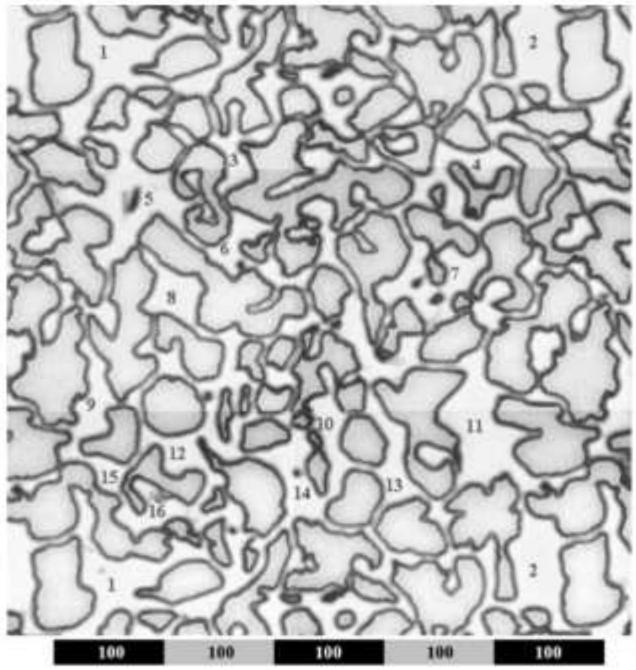

Fig. 3. A composite picture of the micromodel's engraved repetitive pattern (Sirivithayapakorn and Keller, 2003).

The geometry is imported as an SEM image, along with the properties of the pouring medium, such as porosity and permeability. The total model spans 320 and 640 µm. Across the geometry, water flows from right to left. There is no penetration of the solid grains by the flow in the holes. We are aware of the pressures at both the input and output. Assume that there is no flow at the top and bottom limits.

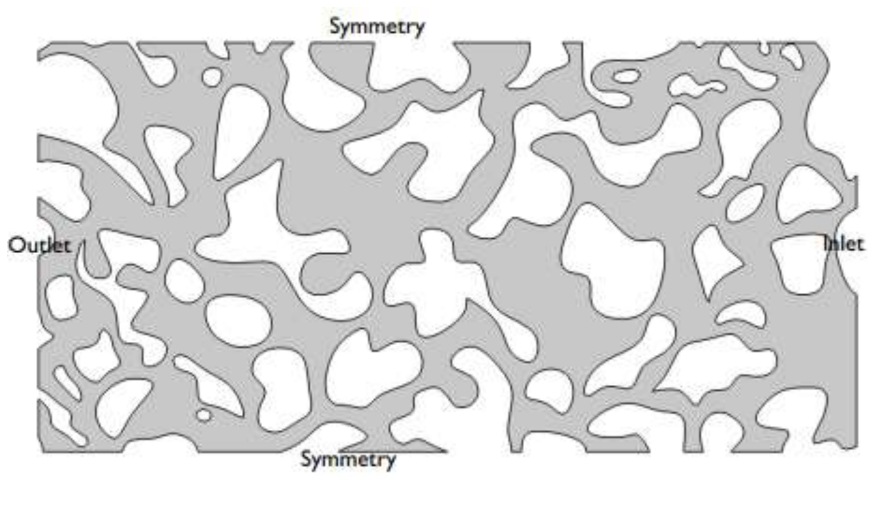

Fig. 4. Geometry and boundary condition.

The maximum Reynolds number is less than 0.01, as the channels are only 0.1 mm wide, and the maximum velocity is less than 10^$^{-4}$ m/s. Instead of using the Laminar Flow interface to solve the Navier-Stokes equation, the example uses the Creeping Flow Interface because the Reynolds number is much less than one. The fluid is thought to have a constant density and be isothermal. This model disregards gravity because of the small-scale issue.

Table 1. Presents the boundary conditions.

Inlet	P_{inlet} =0.715 Pa
Outlet	P_{outlet}= 0 Pa
Fluid density	1000 kg/m^3
Fluid viscosity	0.01 / (m.s)

2.2. Governing Equations

The Creeping Flow interface is used for simulating fluid flows at very low Reynolds numbers for which the inertial term in the Navier-Stokes equations can be neglected. This single-phase flow type, known as Stokes flow, occurs in systems with high viscosity or small geometrical length scales. The equations solved by the Creeping Flow interface are the Stokes equations, which govern the conservation of momentum, and the continuity equation, which governs the conservation of mass.

Furthermore, the Brinkman Equations interface is used to compute fluid velocity and pressure fields of single-phase flow in porous media. The physics interface extends Darcy's law to describe the dissipation of kinetic energy due to viscous shear, similar to the Navier-Stokes equations. Fluids with varying densities can be included at Mach numbers below 0.3. Also, the viscosity of a liquid varies, for example, when describing non-Newtonian fluids. To simplify the equations, select the Stokes-Brinkman flow feature to reduce the dependence on inertial effects when the Reynolds number is significantly less than 1.

2.3. Meshing

Meshing is a computational technique used in engineering, mathematics, and computer graphics to divide a complex structure or domain into smaller, discrete elements, known as mesh elements. These elements, which can be triangles, quadrilaterals, tetrahedra, or other shapes, form a connected network that approximates the geometry of the domain. This discretization enables numerical methods, such as finite element analysis (FEA) and computational fluid dynamics (CFD), to solve physical problems, including stress distribution, heat transport, and fluid flow. To ensure accurate and efficient simulations, meshing turns continuous issues into a form the computer can process.

The outcomes of the analysis depend a lot on how well the mesh is. A fine, dense mesh may yield more precise results, but it will require more time and computing power to achieve this. Conversely, a coarse mesh reduces computational demands but risks less precise solutions. The type of mesh (structured, unstructured, or hybrid) and how it is refined in critical areas are carefully selected based on the analysis requirements. The picture above shows an example of meshing, where a domain is represented as a network of triangular elements that fit perfectly along its complex edges. This shows how to find the right balance between accuracy and ease of use.

Figure 5 shows a 2D mesh structure with an organic, uneven pattern resembling porous or sponge-like shapes. The mesh is composed of triangular pieces that are joined together and come in various sizes and densities to accommodate the uneven and wavy edges of the shapes. The smaller triangles are more focused on tighter curves and edges, which highlight the details of the shape. The larger triangles are used in areas that are more uniform and less complex. The overall structure resembles a web of cells, with empty spaces of various shapes and sizes enclosed by a mesh framework. The black-and-white color scheme makes the difference between the open areas (voids) and the mesh pieces stand out, making it easy to see how the domain is divided up. This type of mesh appears to be well-suited for finite element analysis or simulations in areas with complex shapes.

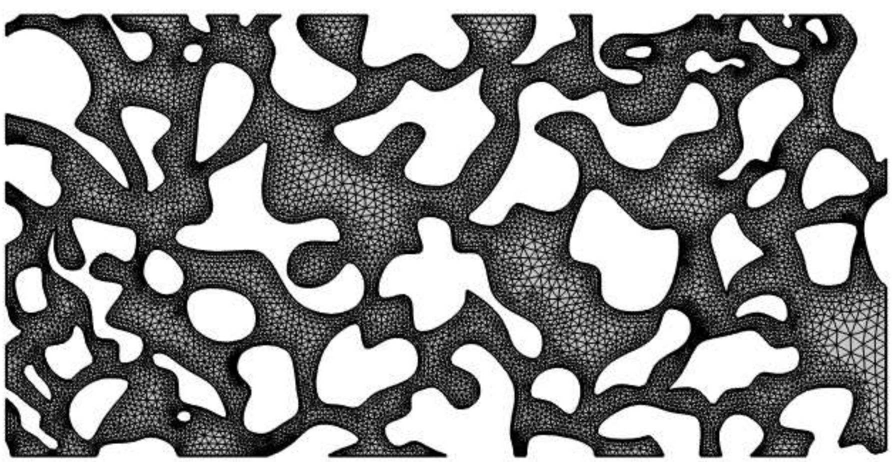

Fig. 5. Meshing.

2.4. Simulation Setup

In this study, COMSOL Multiphysics 6.2 is employed to analyse single-phase fluid flow in porous media. Widely recognized for its versatility in handling diverse porous media applications, COMSOL Multiphysics has been extensively utilized across educational, research, and industrial institutions.

This work utilized both the Creeping Flow interface and Brinkman equations. The stationary physics interface simulates single-phase flow in the pore scale analysis.

3. Results

3.1. Velocity (Creeping Flow Interface)

Figure 6 illustrates the fluid flow through a highly irregular porous medium, where the velocity magnitude and velocity field streamlines are visualized. The surface plot, represented by the background color gradient, shows the velocity magnitude (in m/s) across the porous domain. The scale ranges from 0 (deep blue) to 8×10^{-5} m/s (bright red), clearly showing how the flow velocity varies throughout the medium. High-velocity regions, indicated by red and yellow colors, are primarily concentrated within narrow, tortuous channels that act as preferential flow pathways. Conversely, stagnant flow regions with negligible velocity are represented by large and medium areas that remain dark blue. These inert zones are probably associated with dead-end pores or areas of inadequate connectivity within the porous network.

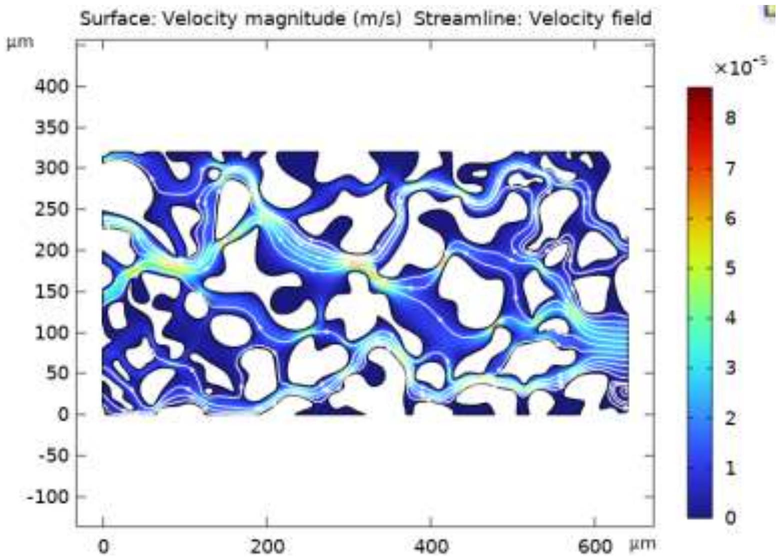

Fig. 6. Shows the velocity profile at the pore scale level.

The white streamlines on top of the velocity surface show how the flow patterns change in the medium. These streamlines indicate the direction of fluid flow and the paths the fluid takes as it moves through the interconnected spaces. In areas with high speeds, the streamlines are thick and closely spaced, resembling small channels where the flow is concentrated. Conversely, in regions of low velocity (dark blue areas), the streamlines become sparse or disappear entirely, indicating areas where the fluid movement is minimal. The smooth and continuous nature of the streamlines suggests laminar flow, which is expected at low velocities in such porous systems.

In addition, the results indicate the complexity of fluid flow through porous media, where the pore structure is responsible for variations in the flow pattern. Efficient flow pathways are indicated by regions with high velocities, whereas slower-moving zones suggest potential inefficiencies that may impact processes such as solute transport, filtration, or catalytic reactions. This visualization illustrates the importance of developing porous materials with optimal pore architectures to enhance flow uniformity and performance in filtration, fuel cells, and oil recovery.

3.2. Pressure Distribution (Creeping Flow Interface)

Figure 7 displays a contour map of the pressure distribution (in Pascals, Pa) within a porous medium, offering detailed insight into how pressure varies spatially across the system. The color gradient represents pressure values, as indicated by the color bar to the right, which spans from 0.39 Pa (deep blue) to 6.91 Pa (red). The contours illustrate the pressure variation along interconnected pore pathways, highlighting the interplay between the geometry of the porous network and fluid flow resistance.

Fig. 7. Presents the pressure distribution at the pore scale level.

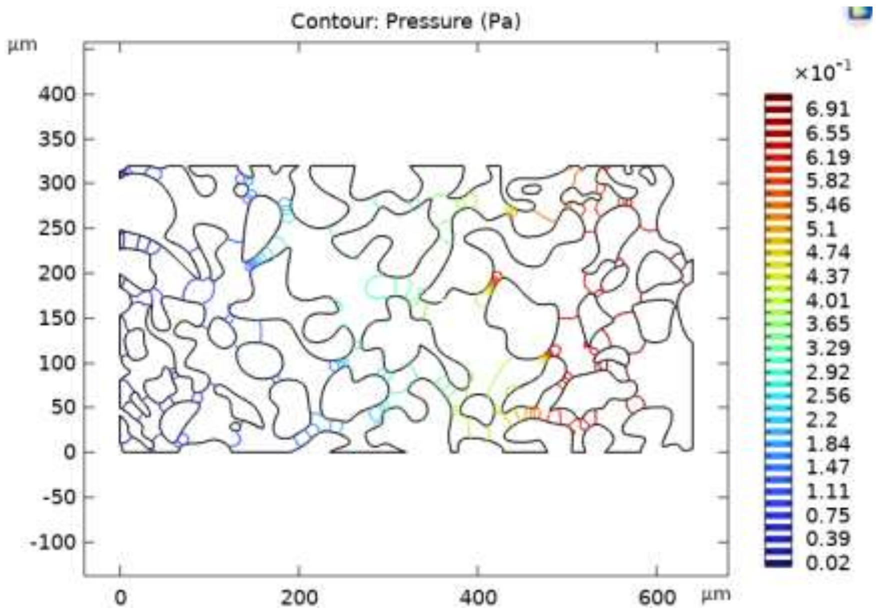

Regions of high pressure (red and orange zones) are concentrated near the right side of the porous medium, where fluid likely enters the system. As the fluid progresses through the interconnected pores, the pressure gradually decreases, transitioning from yellow to green and eventually blue contours toward the outlet side of the medium on the left. This gradient reflects the pressure drop caused by resistance to fluid flow within the complex, tortuous pathways of the porous structure. The pressure drop across the medium directly results from the viscous forces acting on the fluid as it navigates through narrow channels and around solid obstacles.

The pressure contours clearly outline the preferential flow channels where the fluid travels. Narrower channels and constrictions within the medium exhibit sharper pressure gradients (closely spaced contours), indicating higher resistance to flow. These high-gradient regions are critical bottlenecks, where fluid experiences significant energy loss due to the constricted pore geometry. Conversely, broader voids or areas with better connectivity show relatively smooth pressure transitions (widely spaced contours), suggesting lower resistance and more efficient flow.

The overall pressure distribution results from the highly heterogeneous structure of the porous medium. High tortuosity and small constrictions cause significant pressure drop, while broader and more direct routes cause little. This unequal pressure distribution illustrates how pore architecture influences fluid dynamics by creating routes with varying resistance. Dead-end pores also have a minimal effect on the pressure gradient, which supports the idea that they don't play a significant role in fluid movement. The results demonstrate that the shape of the pores is crucial in determining how pressure and fluid flow behave within a porous medium. The steep pressure drop through constricted regions underscores the importance of designing pore networks with optimized connectivity and reduced tortuosity for applications such as filtration and enhanced oil recovery.

3.3. Velocity (Brinkman Equation)

Figure 8 depicts the velocity magnitude and velocity field streamlines for fluid flow through a porous medium. The surface plot displays the velocity magnitude in meters per second (m/s), with values ranging from 0 to 1.8×10^{-5} m/s, as indicated by the color bar on the right. Blue regions correspond to the lowest velocities, while red and yellow regions indicate areas of relatively high velocity. Superimposed on the surface plot are streamlines that trace the flow direction, revealing how fluid navigates through the intricate pore network of the porous medium.

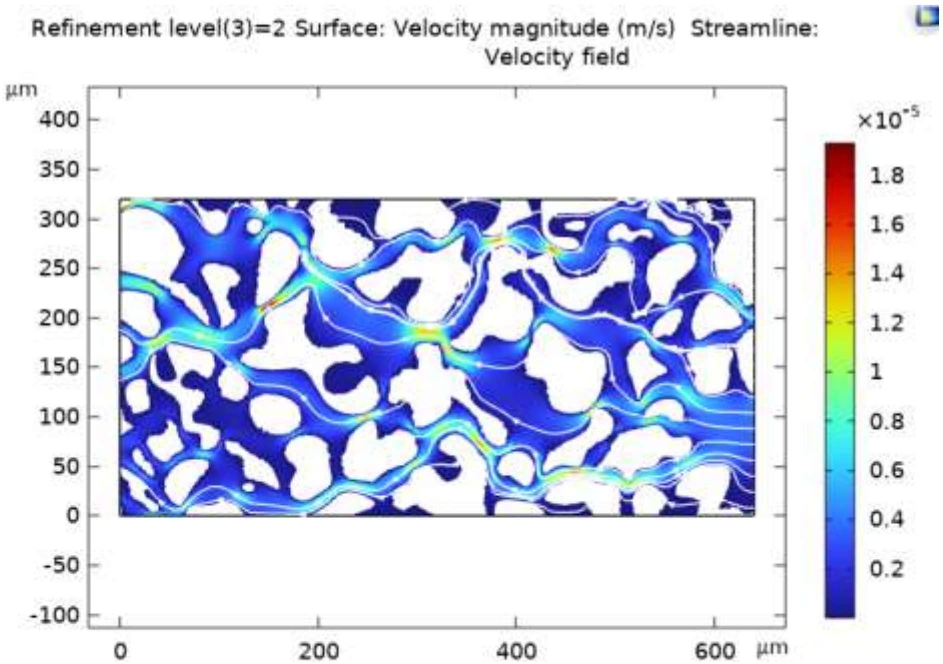

Fig. 8. Illustrates the velocity profile at the pore scale level.

The velocity magnitude varies significantly across the domain due to the heterogeneous geometry of the porous structure. High-velocity regions (red and yellow) are concentrated within narrow, well-connected channels, which act as the primary pathways for fluid transport. These channels facilitate the bulk of the flow, as fluid is forced through these regions of low hydraulic resistance. Low-velocity (dark blue) regions are associated with greater voids or inadequate connections, where fluid stagnates or travels slowly. The velocity distribution shows how pore geometry creates active flow and stagnation zones.

Streamlines illuminate flow dynamics. They are thick in high-velocity locations, especially small channels, indicating flow concentration through these pathways. The streamlines' smooth, continuous character suggests medium laminar flow. Low-velocity regions have sparse or no streamlines, indicating little to no flow. These sluggish areas often have larger voids or dead-end pores, which reduce transfer.

Pore connection and tortuosity also affect flow behavior. A heterogeneous velocity field arises from the tortuous paths of the porous medium, causing the fluid to follow diverse trajectories. According to the continuity equation, narrow medium constrictions increase local velocities, whereas larger, poorly linked portions operate as barriers, raising hydraulic resistance. These flow patterns cause uneven velocity magnitudes, with a few channels dominating. The porous medium's complex structure results in a highly non-uniform velocity field. High-velocity channels dominate fluid transport, while stationary zones show flow distribution inefficiencies.

3.4. Pressure Distribution (Brinkman Equation)

Figure 9 illustrates the pressure distribution within a porous medium using contour lines to map regions of equal pressure. The pressure is measured in Pascals (Pa), with a range from 0.06 Pa (deep blue) to 6.9 Pa (red), as indicated by the color bar on the right. The contour lines indicate how pressure changes across the porous medium at specific points, as well as the density of these lines. This enhanced simulation displays the intricate flow dynamics with high spatial resolution, illustrating how pressure influences the medium's complex shape.

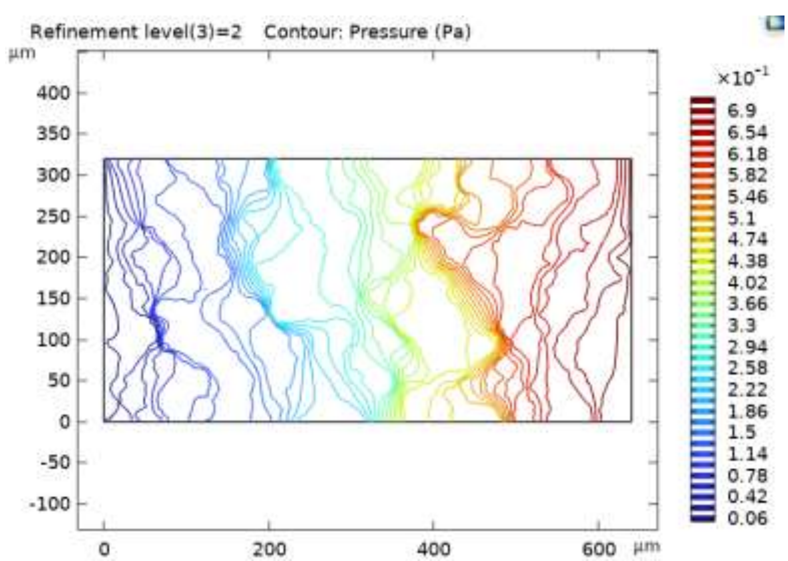

Fig. 9. Shows the velocity profile at the pore scale level.

The pressure distribution follows a transparent gradient from high pressure (red) on the left side to low pressure (blue) on the right. This gradient is a direct consequence of the driving force for fluid flow, where fluid enters at a higher pressure and progressively loses energy as it moves through the medium due to viscous resistance. Narrow, sinuous routes within the porous structure exhibit the steepest pressure drops, as indicated by closely spaced contour lines. The greater flow resistance of these routes causes significant energy losses as fluid constricts.

Broader, less limited paths have smoother pressure shifts and more widely spaced contour lines. Lower resistance zones allow fluid flow more effectively. The steep and shallow pressure gradients show how pore shape affects medium flow resistance. Wider voids relieve flow and reduce pressure drop, while narrower channels produce pressure drop bottlenecks.

The irregular contour lines indicate the tortuosity of the porous structure. As fluid moves through the material, the outlines bend and twist, mirroring its complicated courses. This sinuous flow pattern increases hydraulic resistance and pressure loss between input and output. The pressure contour map illuminates how pore geometry affects medium fluid flow. High resistance and steep pressure gradients indicate fluid transport bottlenecks. Efficient paths with lower resistance have smoother slopes.

4. Discussion

Figure 6, based on the Creeping Flow interface, and Figure 8, a velocity image derived from the Brinkman equation, both depict the velocity magnitude and streamlines within a porous medium. Still, they reflect distinct mathematical approaches and assumptions about flow behavior. These differences result in subtle but meaningful variations in the distribution of velocities, streamline patterns and overall insights into fluid dynamics.

The Creeping Flow model relies on the assumption of negligible inertial forces compared to viscous forces, making it ideal for low Reynolds number flows in tightly packed porous structures. This model strictly adheres to the Stokes flow regime, commonly applied when fluid flow occurs within confined pore spaces, such as in fine-grained soils, biological tissues, or microfluidic devices. The corresponding velocity distribution in the Creeping Flow image highlights narrow channels with concentrated high velocities (yellow and red regions) surrounded by large stagnant zones (deep blue), where velocities are nearly negligible. The streamlines are tightly packed in these narrow channels, indicating laminar flow and high hydraulic resistance due to the medium's tortuosity. The abrupt transitions between high and low velocities emphasize the dominating role of pore geometry in directing fluid transport in this regime.

In contrast, the Brinkman equation introduces an additional term to account for the influence of permeability and the transition from pure Darcy flow to flow regimes where viscous shear effects become significant. The Brinkman equation, therefore, bridges the gap between Stokes flow and Darcy's law, making it suitable for describing flow in porous media with varying pore sizes or intermediate Reynolds numbers. The high-velocity channels remain prominent in the velocity image generated by the Brinkman model. Still, the stagnant zones exhibit slightly higher velocities (lighter blue than the Creeping Flow model). This indicates that the Brinkman equation allows for a smoother velocity distribution, accounting for some shear-driven flow even in regions with lower permeability. The streamlines in the Brinkman image also appear less tightly confined to specific channels, reflecting a more diffused and distributed flow pattern, which is consistent with the added influence of the viscous term.

One difference between the models is the flow resolution in locations with weak pore connections. In the Creeping Flow model, these locations have significantly lower velocities and contribute little to transport. The additional elements in the Brinkman model account for flow over porous material borders and within wider voids, thus resulting in a more gradual decline in velocity. It simulates flow in media with diverse pore diameters or larger permeability contrasts more effectively.

The Creeping Flow model simplifies fluid dynamics, making it ideal for severely confined, low-permeability systems. The Brinkman model represents flow behavior in intermediate permeability or mixed flow regimes more comprehensively. The proper model is needed to predict velocity distributions and transport behavior in microfluidics, filtration, and subsurface flow.

Figures 7 and 9 illustrate the impact of the Creeping Flow interface and Brinkman equation flow models on the pressure gradients in porous media. The precise pore design prevents fluid passage, causing a pressure drop from medium intake to output in both photos. Different assumptions affect the pressure contour resolution, gradient distribution, and flow resistance presentation of the two models.

Inertial forces are negligible in Stokes flow, and viscous forces dominate at the Creeping Flow contact. These assumptions apply to porous systems with very restricted geometries and low Reynolds number flows. Narrow, high-resistance tubes have large pressure gradients. The initial pressure distribution graphic has more detailed pressure outlines. Well-defined porous medium-pressure contours reflect its complex structure. Because flow does not interact with vast stationary zones, pressure gradients, and flow velocities are low. The first image depicts a highly localized pressure distribution with the steepest gradients in flow-conducting channels, exhibiting mild tortuosity and heterogeneity.

The Brinkman equation bridges Darcy's law and the Navier-Stokes equation by incorporating viscous shear in porous media. The second pressure distribution image displays smoother domain pressure gradient outlines that are less confined to flow channels and more uniformly distributed across the medium. Because the Brinkman equation encompasses various flow behaviors, shear-driven flow can occur in low-permeability zones. The smooth pressure contours in the Brinkman image indicate that pressure gradients are dispersed across a wider section of the medium, thereby decreasing the influence of small, high-resistance routes on flow behavior.

The two models treat stagnant or poorly linked regions differently. In the Creeping Flow model, these zones exhibit minimal pressure change and negligible fluid transfer. In the Brinkman model, the added viscous term enables some flow in these areas, resulting in more gradual pressure increases, even in low-permeability or connected zones. This reproduces pressure distribution in media with different pore sizes and flow regimes more accurately.

The Creeping Flow model represents pressure gradients more sharply and locally, making it ideal for Stokes flow in highly confined, low-permeability systems. However, the Brinkman model depicts pressure more evenly and smoothly, capturing flow behavior in locations the Creeping Flow model may miss. This comparison underscores the importance of selecting the appropriate model to accurately predict pressure distribution and flow behavior in porous media applications, including filtration, enhanced oil recovery, and subsurface fluid transport.

5. Conclusions

The pore-scale study of single-phase fluid flow in porous media utilizes advanced numerical methods to overcome the limitations of classic models, such as Darcy's law. The Creeping Flow interface and Brinkman equation demonstrate how pore geometry, viscosity effects, and permeability influence flow behavior.

Simulations show that paths with high-velocity zones (up to 8×10^{-5} m/s) are narrow and interconnected, whereas stagnant sections have negligible flow, indicating structural variability. Brinkman model accommodates viscous shear, resulting in smoother velocity transitions (0 to 1.8×10^{-5} m/s) compared to the Creeping Flow model, which yields steeper gradients. This demonstrates that the Brinkman equation applies to intermediate flow regimes. Pressure drops (0.39–6.91 Pa) in confined areas demonstrate how tortuosity and connectivity impact hydraulic resistance.

The results focus on the need for porous media-specific modeling methodologies. The Creeping Flow model is well-suited for low-permeability, highly confined systems, whereas the Brinkman equation more accurately depicts flow in heterogeneous or mixed-regime environments. These findings have implications for increased oil recovery, groundwater treatment, and pollutant transport, where accurate modeling improves efficiency and sustainability.

This research prepares for future investigations on complex porous systems, including multiphase flows and reactive transport, by combining theoretical modeling with real-world problems. This work enhances our understanding of pore-scale fluid dynamics, enabling petroleum engineers and environmental scientists to design more effective resource management and innovative engineering solutions.

References

Anvari, S., Turzó, Z., 2022. Application of Nanotechnology in Enhanced Oil Recovery. Geosci. Eng. 10, 185–201. https://doi.org/10.33030/geosciences.2022.15.185

Asim, T., Hawez, H.K., 2024. Effects of CO2 Geosequestration on Opalinus Clay. Energies 17. https://doi.org/10.3390/en17102431

Auset, M., Keller, A.A., 2004. Pore-scale processes that control dispersion of colloids in saturated porous media. Water Resour. Res. 40. https://doi.org/10.1029/2003WR002800

Blunt, M.J., 2001. Flow in porous media - Pore-network models and multiphase flow. Curr. Opin. Colloid Interface Sci. 6, 197–207. https://doi.org/10.1016/S1359-0294(01)00084-X

Carrillo, F.J., Bourg, I.C., Soulaine, C., 2020. Multiphase flow modeling in multiscale porous media: An open-source micro-continuum approach. J. Comput. Phys. X 8, 100073.

https://doi.org/10.1016/j.jcpx.2020.100073

Egya, D.O., Geiger, S., Corbett, P.W.M., March, R., Bisdom, K., Bertotti, G., Bezerra, F.H., 2019. Analysing the limitations of the dual-porosity response during well tests in naturally fractured reservoirs. Pet. Geosci. 25, 30–49. https://doi.org/10.1144/petgeo2017-053

Ekechukwu, O.M., Asim, T., Hawez, H.K., 2024. Recent Developments in Hydrocyclone Technology for Oil-in-Water Separation from Produced Water. Energies 17. https://doi.org/10.3390/en17133181

Figueiredo, B., Tsang, C.F., Rutqvist, J., Niemi, A., 2015. A study of changes in deep fractured rock permeability due to coupled hydro-mechanical effects. Int. J. Rock Mech. Min. Sci. 79, 70–85. https://doi.org/10.1016/j.ijrmms.2015.08.011

Fopa, R.D., Bianco, C., Archilha, N.L., Moreira, A.C., Pak, T., 2023. A pore-scale investigation of the effect of nanoparticle injection on properties of sandy porous media. J. Contam. Hydrol. 253, 104126. https://doi.org/10.1016/j.jconhyd.2022.104126

Harting, J., Chin, J., Venturoli, M., Coveney, P. V., 2005. Large-scale lattice Boltzmann simulations of complex fluids: Advances through the advent of computational Grids. Philos. Trans. R. Soc. A Math. Phys. Eng. Sci. 363, 1895–1915. https://doi.org/10.1098/rsta.2005.1618

Hawez, H., Ahmed, Z., 2014. Enhanced oil recovery by CO2 injection in carbonate reservoirs. WIT Trans. Ecol. Environ. 186, 547–558. https://doi.org/10.2495/ESUS140481

Hawez, H., Sanaee, R., Faisal, N.H., 2021. Multiphase Flow Modelling in Fractured Reservoirs using a Novel Computational Fluid Dynamics Approach, in: Paper Presented at the 55th U.S. Rock Mechanics/Geomechanics Symposium,. Virtual. https://doi.org/ARMA-2021-1077

Hawez, H.K., Asim, T., 2024a. Effects of Externally Applied Stress on Multiphase Flow Characteristics in Naturally Fractured Tight Reservoirs. Appl. Sci. 14, 8540. https://doi.org/10.3390/app14188540

Hawez, H.K., Asim, T., 2024b. Impact of Regional Pressure Dissipation on Carbon Capture and Storage Projects: A Comprehensive Review. Energies 17, 1889. https://doi.org/10.3390/en17081889

Hawez, H.K., Asim, T., Fazio, M., 2024. A Fully Coupled Model for Predicting Geomechanical and Multiphase Flow Behaviour in Fractured Rocks. Unconv. Resour. 100105. https://doi.org/10.1016/j.uncres.2024.100105

Hawez, H.K., Sanaee, R., Faisal, N.H., 2021. A critical review on coupled geomechanics and fluid flow in naturally fractured reservoirs. J. Nat. Gas Sci. Eng. 95. https://doi.org/10.1016/j.jngse.2021.104150

Herrera-Hernández, E.C., Aguilar-Madera, C.G., Espinosa-Paredes, G., Hernández, D., 2023. Modeling single-phase fluid flow in porous media through non-local fractal continuum equation. J. Eng. Math. 138, 1–18. https://doi.org/10.1007/s10665-022-10245-4

Hughes, R.G., Blunt, M.J., 2001. Network modeling of multiphase flow in fracture. Adv. Water Resour. 24, 409–421. https://doi.org/10.1016/S0309-1708(00)00064-6

Jettestuen, E., Helland, J.O., Prodanovič, M., 2013. A level set method for simulating capillary-controlled displacements at the pore scale with nonzero contact angles. Water Resour. Res. 49, 4645–4661. https://doi.org/10.1002/wrcr.20334

Joekar-Niasar, V., van Dijke, M.I.J., Hassanizadeh, S.M., 2012. Pore-Scale Modeling of Multiphase Flow and Transport: Achievements and Perspectives. Transp. Porous Media 94, 461–464. https://doi.org/10.1007/s11242-012-0047-4

Kumar, M., Guasto, J.S., Ardekani, A.M., 2022. Transport of complex and active fluids in porous media. J. Rheol. (N. Y. N. Y). 66, 375–397. https://doi.org/10.1122/8.0000389

Liu, Z., Wu, H., 2016. Pore-scale modeling of immiscible two-phase flow in complex porous media. Appl. Therm. Eng. 93, 1394–1402. https://doi.org/10.1016/j.applthermaleng.2015.08.099

Menke, H.P., Gao, Y., Linden, S., Andrew, M.G., 2022. Using Nano-XRM and High-Contrast Imaging to Inform Micro-Porosity Permeability During Stokes–Brinkman Single and Two-Phase Flow Simulations on Micro-CT Images. Front. Water 4, 1–17. https://doi.org/10.3389/frwa.2022.935035

Montessori, A., Prestininzi, P., La Rocca, M., Falcucci, G., Succi, S., Kaxiras, E., 2016. Effects of Knudsen diffusivity on the effective reactivity of nanoporous catalyst media. J. Comput. Sci. 17, 377–383. https://doi.org/10.1016/j.jocs.2016.04.006

Rabbani, A., Fernando, A.M., Shams, R., Singh, A., Mostaghimi, P., Babaei, M., 2021. Review of Data Science Trends and Issues in Porous Media Research With a Focus on Image-Based Techniques. Water Resour. Res. 57, 1–44. https://doi.org/10.1029/2020WR029472

Singh, K., Menke, H., Andrew, M., Lin, Q., Rau, C., Blunt, M.J., Bijeljic, B., 2017. Dynamics of snap-off and pore-filling events during two-phase fluid flow in permeable media. Sci. Rep. 7, 1–13. https://doi.org/10.1038/s41598-017-05204-4

Sirivithayapakorn, S., Keller, A., 2003. Transport of colloids in saturated porous media: A pore-scale observation of the size exclusion effect and colloid acceleration. Water Resour. Res. 39. https://doi.org/10.1029/2002WR001583

Sivapalan, M., Blöschl, G., 2015. Time scale interactions and the coevolution of humans and water. Water Resour. Res. 51, 6988–7022. https://doi.org/10.1002/2015WR017896

Sochi, T., 2010. Pore-Scale Modeling of Non-Newtonian Flow in Porous Media.

Soulaine, C., Roman, S., Kovscek, A., Tchelepi, H.A., 2018. Pore-scale modelling of multiphase reactive flow: Application to mineral dissolution with production of CO2. J. Fluid Mech. 855, 616–645. https://doi.org/10.1017/jfm.2018.655

Sun, K., Liu, H., Leung, J.Y., Wang, J., Feng, Y., Liu, R., Kang, Z., Zhang, Y., 2024. Impact of effective stress on permeability for carbonate fractured-vuggy rocks. J. Rock Mech. Geotech. Eng. 16, 942–960. https://doi.org/10.1016/j.jrmge.2023.04.007

Wu, Y., Tahmasebi, P., Liu, K., Fagbemi, S., Lin, C., An, S., Ren, L., 2022. Two-phase flow in heterogeneous porous media: A multiscale digital model approach. Int. J. Heat Mass Transf. 194, 123080. https://doi.org/10.1016/j.ijheatmasstransfer.2022.123080

Young, A.H., Kabala, Z.J., 2024. Hydrodynamic Porosity: A New Perspective on Flow through Porous Media, Part II. Water (Switzerland) 16. https://doi.org/10.3390/w16152166

Zheng, X., Mahabadi, N., Yun, T.S., Jang, J., 2017. Effect of capillary and viscous force on CO2 saturation and invasion pattern in the microfluidic chip. J. Geophys. Res. Solid Earth 122, 1634–1647. https://doi.org/10.1002/2016JB013908